International Journal of Plasticity 26 (2010) 1629–1644

Contents lists available at ScienceDirect

International Journal of Plasticity

journal homepage: www.elsevier.com/locate/ijplas

Effects of intergrain sliding on crack growth in nanocrystalline materials

S.V. Bobylev [a], A.K. Mukherjee [b], I.A. Ovid'ko [a,*], A.G. Sheinerman [a]

[a] Institute of Problems of Mechanical Engineering, Russian Academy of Sciences, Bolshoj 61, Vasil. Ostrov, St. Petersburg 199178, Russia
[b] Department of Chemical Engineering and Materials Science, University of California, Davis, 1 Shields Avenue, Davis, CA 95616, USA

ARTICLE INFO

Article history:
Received 11 June 2009
Received in final revised form 8 March 2010
Available online 19 March 2010

Keywords:
Cracks
Nanomaterials
Dislocations

ABSTRACT

Theoretical models are suggested which describe the effects of intergrain sliding on crack growth in nanocrystalline metals and ceramics. Within the models, stress concentration near cracks initiates intergrain sliding which is non-accommodated at low temperatures and effectively accommodated at intermediate temperatures. The first model is focused on the non-accommodated intergrain sliding which leads to generation of dislocations at triple junctions of grain boundaries. These dislocations cause partial stress relaxation in the vicinities of crack tips and thereby hamper crack growth. It is shown that the non-accommodated intergrain sliding increases fracture toughness by 10–30% in nanocrystalline Al, Ni and 3C–SiC. The second model deals with the case of intermediate temperatures. Within this model, intergrain sliding is effectively accommodated by diffusion-controlled climb of grain boundary dislocations. The accommodated intergrain sliding in nanocrystalline materials results in crack blunting which, in its turn, leads to an increase (by a factor ranging from 1.1 to around 3, depending on temperature) of fracture toughness.

1. Introduction

The outstanding mechanical properties of nanocrystalline metals and ceramics represent the subject of rapidly growing research efforts motivated by a wide range of their applications (see, e.g., Khan et al., 2000, 2006, 2008a,b; Khan and Zhang, 2000; Mukherjee, 2002; Kumar et al., 2003a; Gutkin and Ovid'ko, 2004; Kuntz et al., 2004; Xia et al., 2004; Ovid'ko, 2005, 2007; Weissmüller and Markmann, 2005; Wolf et al., 2005; Meyers et al., 2006; Warner et al., 2006; Xu et al., 2006; Capolungo et al., 2007; Dao et al., 2007; Koch, 2007; Koch et al., 2007; Aifantis, 2009; Barai and Weng, 2009; Bobylev et al., 2009; Farrok and Khan, 2009; Figueiredo et al., 2009). In most cases, nanocrystalline materials have superior strength and hardness but at the expenses of both low tensile ductility and low fracture toughness; see reviews (Mukherjee, 2002; Kumar et al., 2003a; Kuntz et al., 2004; Ovid'ko, 2005, 2007; Wolf et al., 2005; Meyers et al., 2006; Dao et al., 2007; Koch, 2007) and book (Koch et al., 2007). Low ductility and low toughness are highly undesired for structural applications of nanocrystalline materials. In particular, low fracture toughness of nanocrystalline ceramics, as with their conventional microcrystalline ceramics, is treated as the key factor limiting their practical utility (Kuntz et al., 2004). In these circumstances, there is large interest in understanding the fundamental laws governing crack growth processes in nanocrystalline materials.

The tendency of nanocrystalline materials to show low ductility and toughness is well illustrated by the experimental fact that some nanocrystalline metals with the face-centered-cubic lattice (hereinafter called fcc metals) exhibit a ductile-to-brittle transition with decreasing grain size (Li and Ebrahimi, 2004, 2005; Ebrahimi et al., 2006). In contrast, good ductility and toughness are always inherent to coarse-grained fcc metals where emission of lattice dislocations from cracks causes effective blunting of cracks and thus suppresses their growth. The difference in fracture behavior between nanocrystalline and

* Corresponding author. Tel.: +7 812 321 4764; fax: +7 812 321 4771.
E-mail address: ovidko@def.ipme.ru (I.A. Ovid'ko).

0749-6419/$ - see front matter © 2010 Elsevier Ltd. All rights reserved.
doi:10.1016/j.ijplas.2010.03.001

coarse-grained fcc metals can be attributed to the difference in deformation modes dominating in these materials. The lattice dislocation slip serves as the dominant deformation mode in conventional coarse-grained metals in wide temperature ranges and microcrystalline ceramics at elevated temperatures. However, when the grain size of a material decreases down to the nanometer scale, the lattice dislocation slip is suppressed (Mukherjee, 2002; Kumar et al., 2003a; Kuntz et al., 2004; Ovid'ko, 2005, 2007; Wolf et al., 2005; Meyers et al., 2006; Dao et al., 2007; Koch, 2007; Koch et al., 2007) because grain boundaries (GBs) (whose amount is very large in nanocrystalline materials) stop gliding lattice dislocations. At the same time, alternative deformation modes such as intergrain sliding, Coble creep, triple junction diffusional creep, rotational deformation and nanoscale twin deformation effectively operate in nanocrystalline metals and ceramics (Mukherjee, 2002; Kumar et al., 2003a; Kuntz et al., 2004; Ovid'ko, 2005, 2007; Wolf et al., 2005; Meyers et al., 2006; Dao et al., 2007; Koch, 2007; Koch et al., 2007).

The alternative deformation modes can play the role of specific toughening micromechanisms in nanocrystalline materials, when the conventional toughening associated with the lattice slip is suppressed. This idea is in agreement with experimental data showing enhancement of fracture toughness of several nanocrystalline ceramics (Bhaduri and Bhaduri, 1997; Kuntz et al., 2004; Zhao et al., 2004; Kaminskii et al., 2005; Pei et al., 2005) and nanocrystalline nickel (Mirshams et al., 2001), compared to that of their microcrystalline counterparts. The discussed idea and experimental data (Bhaduri and Bhaduri, 1997; Mirshams et al., 2001; Kuntz et al., 2004; Zhao et al., 2004; Kaminskii et al., 2005; Pei et al., 2005) serve as the basis of theoretical models of specific micromechanisms hampering crack growth in nanocrystalline materials. In particular, recently, nanoscale twin deformation carried by partials emitted from grain boundaries (Gutkin et al., 2008a,b) and stress-driven migration of grain boundaries (Ovid'ko et al., 2008) have been theoretically revealed to be specific toughening micromechanisms in nanocrystalline ceramics and metals. Besides, creep deformation conducted by grain boundary processes (Ashby–Verall creep carried by intergrain sliding accommodated by GB diffusion and grain rotations (Ashby and Verall, 1973; Yang and Wang, 2004)) was suggested as a toughening micromechanism providing crack blunting (at grain size scales of 10 nm or more) in nanocrystalline metals (Yang and Wang, 2008; Yang and Yang, 2009). However, the creep deformation considered by Yang and Wang (2008) and Yang and Yang (2009) is a diffusion-controlled process which can effectively contribute to toughening of nanocrystalline metals only in the limiting partial cases where diffusion is very fast (at high temperatures) and/or crack growth is extremely slow. We think that intergrain sliding can effectively contribute to toughening of nanocrystalline ceramics and metals in a situation with comparatively wide ranges of crack tip velocity and temperature. The main aim of this paper is to theoretically describe the effects of intergrain sliding on crack growth in nanocrystalline metals and ceramics at low and intermediate temperatures. In the former case, the focuses will be placed on the intergrain-sliding-induced formation of dislocations at triple junctions of GBs and their role in partial stress relaxation in the vicinities of crack tips. In the case of intermediate temperatures, we theoretically examine crack blunting which occurs at nanoscopic scales (close to 1–10 nm) and is related to intergrain sliding effectively accommodated by diffusion-controlled climb of GB dislocations. Finally, with the results of the models describing the effects of non-accommodated and accommodated intergrain sliding processes on crack growth in nanocrystalline metals and ceramics, we will consider the sensitivity of fracture toughness of these materials to their grain size. Also, the influence of non-equilibrium GBs on toughness of nanocrystalline metals will be briefly discussed.

2. Intergrain sliding near crack tips in nanocrystalline metals and ceramics

The lattice dislocation slip in nanocrystalline metallic and ceramic materials with finest grains ($d < d' \approx 20$ nm) is suppressed (Mukherjee, 2002; Kumar et al., 2003a; Kuntz et al., 2004; Ovid'ko, 2005, 2007; Wolf et al., 2005; Meyers et al., 2006; Dao et al., 2007; Koch, 2007; Koch et al., 2007). The same is valid for nanocrystalline ceramics with intermediate grains (with the sizes $d < 100$ nm) and conventional microcrystalline ceramics at low and intermediate temperatures at which large Peierls barriers suppress lattice dislocation slip. In these materials, GB-conducted deformation modes (Mukherjee, 2002; Kumar et al., 2003a; Kuntz et al., 2004; Ovid'ko, 2005, 2007; Wolf et al., 2005; Meyers et al., 2006; Dao et al., 2007; Koch, 2007; Koch et al., 2007) and twin deformation (commonly carried by partials generated at GBs) (Chen et al., 2003; Liao et al., 2003; Wang et al., 2005; Zhu et al., 2005; Wu and Zhu, 2008; Zhu et al., 2009) come into play. Among GB-conducted deformation modes, intergrain sliding is treated to be crucially important in nanocrystalline metals and ceramics in certain situations. In particular, intergrain sliding processes are experimentally shown to play the dominant role in superplastic deformation of nanocrystalline metallic and ceramic materials (Mukherjee, 2002; Xu et al., 2006; Koch et al., 2007). Computer simulations (Van Swygenhoven et al., 1999; Van Swygenhoven and Derlet, 2001; Farkas and Curtin, 2005; Monk et al., 2006) highlighted the role of intergrain sliding as one of the key mechanisms of plastic deformation in nanocrystalline metals, especially at very high stresses and strain rates (see also review by Wolf et al. (2005) and references therein). Also, the mechanical behavior of nanocrystalline ceramics is strongly influenced by GB deformation processes in amorphous GBs often existing in such materials; see, e.g., experimental data (Kuntz et al., 2004; Xu et al., 2006; Dominguez-Rodriguez et al., 2007; Hulbert et al., 2007) and computer simulations (Szlufarska et al., 2005; Mo and Szlufarska, 2007). For instance, following the computer simulations (Szlufarska et al., 2005; Mo and Szlufarska, 2007) of the evolution of the nanocrystalline cubic phase of silicon carbide (3C–SiC) under a mechanical load, plastic deformation intensively occurs within amorphous GBs in these nanocrystalline ceramics. In the present and next sections we theoretically examine the role of GBs as toughening structural elements in nanocrystalline metals and ceramics.

Let us consider a nanocrystalline specimen with a mode I crack under tensile deformation (Fig. 1). The crack tip is assumed to be located at a GB. High local stresses operating near the crack trip can initiate intergrain sliding (Fig. 1). In its turn, the processes of intergrain sliding in nanocrystalline materials are capable of producing edge dislocations at triple junctions (Bobylev et al., 2009). Here we consider the situation where intergrain sliding occurs in a part of the boundary, located between the crack tip and a triple junction, and results in the formation of an edge dislocation located at the triple junction nearest to the crack tip, as shown in Fig. 1. The dislocation creates stresses that influence crack growth. This process is expected to be specific precisely for nanocrystalline solids, because they are specified by very large volume fractions occupied by both boundaries and their triple junctions. Amounts of GBs in conventional polycrystals are low, in which case one can commonly neglect the effects of intergrain sliding on crack growth.

Intergrain boundary sliding means a shear of neighboring grains with respect to each other, which is localized in their GBs. From a microscopic viewpoint, intergrain boundary sliding is treated to occur by either movement of GB dislocations or local shear events (Sutton and Balluffi, 1996; Conrad and Narayan, 2000; Van Swygenhoven and Derlet, 2001; Gutkin and Ovid'ko, 2004; Padmanabhan and Gleiter, 2004; Bobylev et al., 2006). In particular, the sliding along GBs with translationally ordered structures can be effectively conducted by movement of gliding GB dislocations with Burgers vectors parallel with corresponding boundary planes (Sutton and Balluffi, 1996; Gutkin and Ovid'ko, 2004).

Besides the dislocation description (Sutton and Balluffi, 1996; Gutkin and Ovid'ko, 2004) of intergrain sliding, there is an alternative view (Sutton and Balluffi, 1996; Conrad and Narayan, 2000; Van Swygenhoven and Derlet, 2001; Padmanabhan and Gleiter, 2004; Demkowicz et al., 2007) that such sliding in coarse-grained and nanocrystalline solids occurs by local shear events, thermally activated and driven by the shear stress. Local shear events represent either individual atomic jumps or local transformations of small groups of atoms in the grain boundary phase. This approach, in fact, is based on the theory (Argon, 1979) of thermally activated and shear-stress-driven local shear events carried by free-volume defects in plastically deformed metallic glasses. In this context, intergrain sliding by local shear events is expected to be dominant in non-equilibrium GBs with disordered structures and amorphous GBs.

The structure of GBs in nanocrystalline metallic materials fabricated by severe plastic deformation and other highly non-equilibrium methods is commonly non-equilibrium, with high densities of disorderedly arranged GB defects (Valiev and Alexandrov, 1999; Valiev et al., 2000; Huang et al., 2001; Valiev, 2004; Koch et al., 2007). Nanocrystalline ceramics, as with their conventional microcrystalline counterparts (Clarke, 1987), often contain amorphous GBs (Kuntz et al., 2004; Xu et al., 2006; Dominguez-Rodriguez et al., 2007; Hulbert et al., 2007). In these circumstances, hereinafter, we will focus our

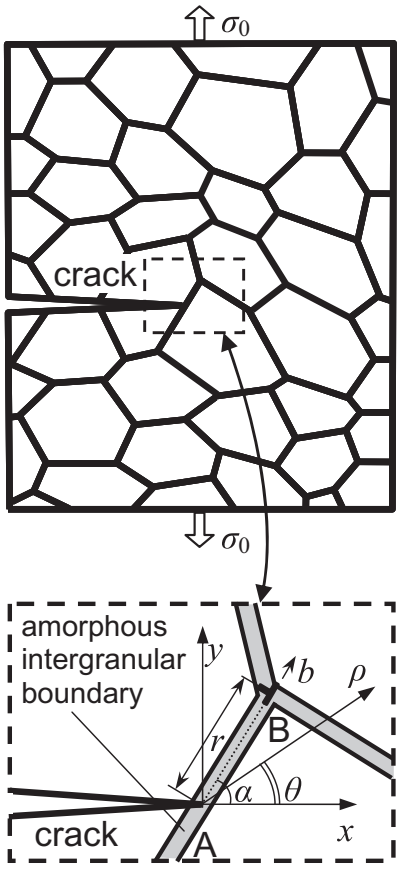

Fig. 1. Crack in a deformed nanocrystalline solid. The magnified inset highlights generation of an edge dislocation at the boundary (grain boundary or amorphous intergranular boundary) near the tip of a long crack that intersects the boundary.

consideration on intergrain sliding through local shear events in non-equilibrium and amorphous GBs in nanocrystalline metals and ceramics.

Within our model, the dislocation (Fig. 1) results from intergrain sliding that occurs through local shear events in either a non-equilibrium, or an amorphous GB in a nanocrystalline specimen. In this case, the Burgers vector magnitude of each dislocation at a boundary gradually grows (due to the accumulation of local shear events) in parallel with local plastic strain carried by intergrain sliding in this boundary; for details, see Bobylev et al. (2009). The direction of the dislocation Burgers vector is parallel with the boundary line (plane in the three-dimensional case). Such dislocations are treated in terms of the Volterra theory of dislocations in continuum media (Volterra, 1907; Hirth and Lothe, 1982) as dislocation-like sources of internal stresses, but not conventional lattice dislocations. In doing so, such dislocations are commonly immobile at the triple junctions of amorphous GBs (Fig. 1). (Note that the notion of such non-crystallographic dislocations with continuously growing Burgers vector magnitudes has recently been used in a description of plastic deformation in nanocrystalline materials (Gutkin and Ovid'ko, 2006, 2008), nanowires (Bobylev and Ovid'ko, 2009) and Gum Metals (Gutkin et al., 2006, 2008a, b) where such non-crystallographic dislocations have been observed in "in situ" experiments (Cui et al., 2009).)

In general, intergrain sliding near a crack tip can occur as either a non-accommodated or an accommodated process. The non-accommodated intergrain sliding occurs at comparatively low temperatures ($T < T_{GBD}$) at which GB diffusion is suppressed. (For instance, GB diffusion in metals is treated to be suppressed at low homologous temperatures $T < T_{GBD} = 0.3T_m$, where T_m is the melting temperature (Vladimirov, 1975).) The non-accommodated intergrain sliding results in the generation of a Volterra dislocation (Fig. 1). At the same time, the intergrain sliding can occur in parallel with such accommodation processes as diffusion-controlled climb of grain boundary dislocations, dislocation emission within the grain interior and associated creation of grain boundary ledges. Intergrain sliding accommodated by diffusion based processes is expected to intensively occur in nanocrystalline materials in the temperature range $T_{GBD} < T < T_{GG}$, where T_{GG} is the temperature at which intensive grain growth (destroying the nanocrystalline structure) occurs. The dislocation emission within the grain interior effectively comes into play in materials with enhanced lattice slip, e.g., metallic materials with low Peierls stress in wide temperature range and ceramic materials at high temperatures at which thermally activated lattice slip overcomes large Peierls barrier. The discussed representations on generation of dislocations at triple junctions due to intergrain sliding and their transformations into lattice dislocations in nanocrystalline materials are in agreement with "in situ" experimental observation (Kumar et al., 2003b) of lattice dislocation emission from triple junctions in deformed nanocrystalline Ni foils and similar observations based on computer simulations (Van Swygenhoven et al., 2002; Farkas et al., 2005).

The main effect of non-accommodated intergrain sliding processes on crack growth in nanocrystalline materials is in generation of triple junction dislocations whose stress fields release, in part, high local stresses near crack tips. The accommodated intergrain sliding causes blunting of crack tips, and this process hampers crack growth. These effects of non-accommodated and accommodated intergrain sliding processes on crack growth in nanocrystalline materials will be considered in detail in Sections 3 and 4, respectively.

3. Effect of non-accommodated intergrain sliding on fracture toughness of nanocrystalline metals and ceramics at low temperatures

Consider a nanocrystalline solid consisting of nanoscale grains divided by GBs and containing a long flat crack of length l. The solid is under tensile load at low temperature ($T < T_{GBD}$). A two-dimensional section of a typical fragment of the solid is schematically shown in Fig. 1. Let the crack intersect the boundary at the point distant by r_0 ($r_0 << l$) from the nearest triple junction (Fig. 1). The local stresses near the crack tip in the solid under a tensile load initiate intergrain sliding through local shear events along the GB AB (Fig. 1) and other GBs in the vicinity of the tip. Since GBs end at triple junctions, such junctions serve as natural geometric obstacles for intergrain sliding in nanocrystalline and microcrystalline materials (see, e.g., Fedorov et al., 2003; Ruano et al., 2003; Bobylev et al., 2006, 2009; Mohamed and Chauhan, 2006; Mohamed, 2007). In particular, triple junction B obstructs intergrain sliding along GB AB (Fig. 1), because the conditions for lattice dislocation slip (slip plane orientation, Burgers vector magnitude for lattice dislocations, stress characterizing resistance to plastic shear (the Peierls stress), etc.) in grain I are different from those for intergrain sliding along GB AB. In these circumstances, following standard representations on intergrain sliding (Fedorov et al., 2003; Ruano et al., 2003; Bobylev et al., 2006, 2009; Mohamed and Chauhan, 2006; Mohamed, 2007), the unfinished plastic shear associated with intergrain sliding is accumulated at and near the triple junction B. In terms of the theory of defects in solids, the triple junction B contains a dislocation (Fig. 1) whose Burgers vector magnitude gradually grows with rising the unfinished plastic shear associated with intergrain sliding (Bobylev et al., 2009).

In this section, we consider the situation where triple junction dislocations generated due to intergrain sliding are immobile (Fig. 1). This situation is realized, if the Peierls stress for lattice dislocation slip is very high, and deformation occurs at low homologous temperatures ($T < T_{GBD}$) at which GB diffusion and thereby GB-diffusion-controlled climb of GB dislocations are suppressed. In doing so, the limiting value b_c of the Burgers vector magnitude of the triple junction dislocation near a crack tip (Fig. 1) is controlled by the external stress and its effect on crack growth. Following the estimates given in this section (see below), the limiting value b_c ranges approximately from 0.1 to 0.6 nm, depending on the material.

Let us consider a triple junction dislocation (produced by the non-accommodated intergrain sliding along GB AB; see Fig. 1) and its effect on the fracture toughness of a nanocrystalline solid. To do so, we will use the standard crack growth

criterion (Irwin, 1957) based on the balance between the driving force related to a decrease in the elastic energy and the hampering force related to the formation of a new free surface during crack growth. This criterion is given as (Irwin, 1957):

$$\frac{1-\nu}{2G}(K_I^2+K_{II}^2)=2\gamma, \tag{1}$$

where γ is the specific energy of the new free surface (per its unit area), K_I and K_{II} are the intensity factors for normal (to the crack line in the two-dimensional case) and shear stresses, respectively. In the considered situation where the crack growth direction is perpendicular to the direction of the external load, the coefficients K_I and K_{II} are given as:

$$\begin{aligned} K_I &= K_I^{\sigma}+k_I^d,\\ K_{II} &= k_{II}^d. \end{aligned} \tag{2}$$

Here K_I^{σ} is the intensity factor for the external stress σ_0, while k_I^d and k_{II}^d are the intensity factors for the stresses created by the edge dislocation located near the crack tip (Fig. 1).

Within the macroscopic mechanical description, the effect of the local plastic flow (intergrain sliding resulting in the formation of a dislocation) on crack growth can be accounted for through the introduction of the effective fracture toughness K_{IC}^*. In this case, the crack is considered as that propagating under the action of the tensile load perpendicular to the crack growth direction, while the presence of the dislocation just changes the value of K_{IC}^* compared to the case of brittle crack propagation. In these circumstances, the critical condition for the crack growth can be represented as (see, e.g., Panasyuk, 1988): $K_I^{\sigma}=K_{IC}^*$.

With expressions (2) substituted to formula (1) and the critical condition $K_I^{\sigma}=K_{IC}^*$ taken into account, one finds the following expression for the factor K_{IC}^*:

$$K_{IC}^*=\sqrt{\frac{4G\gamma}{1-\nu}-(k_{II}^d)^2}-k_I^d. \tag{3}$$

In order to characterize the effect of dislocations produced by intergrain sliding (Fig. 1) on crack growth, one should compare the value K_{IC}^* with the fracture toughness $K_{IC}=\sqrt{4G\gamma/(1-\nu)}$ in the dislocation-free case, that is, the case of brittle fracture with the intergrain sliding being completely suppressed.

Let us calculate the effective fracture toughness K_{IC}^* in the situation where the dislocation is located near the crack, as shown in Fig. 1. In doing so, b denotes the Burgers vector magnitude of the dislocation, r_0 the distance between the dislocation and the crack tip, θ the angle made by the boundary plane (or the dislocation Burgers vector) and the coordinate axis Ox. The stress intensity factors k_I^d and k_{II}^d for the dislocation-induced stresses are calculated by Zhang and Li (1991). They are given as:

$$k_I^d=-\frac{3\pi Db\sin\theta\cos(\theta/2)}{\sqrt{2\pi r_0}},\quad k_{II}^d=-\frac{3\pi Db[\cos(\theta/2)+3\cos(3\theta/2)]}{2\sqrt{2\pi r_0}}, \tag{4}$$

where $D=G/[2\pi(1-\nu)]$.

In our model, the Burgers vector magnitude b, figuring in formulas (4), is arbitrary, because the magnitude b characterizes a non-crystallographic dislocation (for details, see Bobylev et al., 2009). In the quasi-equilibrium state, the Burgers vector magnitude b corresponds to a minimum of the energy change ΔW associated with the dislocation generation process (Fig. 1). In the situation under consideration, the energy change ΔW has three terms:

$$\Delta W=W_s+W_c-A. \tag{5}$$

Here W_s is the proper elastic energy of the dislocation; W_c is the dislocation core energy, and A denotes the work of the shear stress, spent to generation of the dislocation.

Since the dislocation (Fig. 1) is located near the crack free surface, its stresses are screened. The proper energy of such a dislocation is calculated with the aid of the formula (Lin and Thomson, 1986) taking into account the image forces that characterize the screening effect. In doing so, we have:

$$W_s\approx\frac{Db^2}{2}\ln\frac{r}{r_c}. \tag{6}$$

Here r_c is the dislocation core radius. The dislocation core energy W_c in the standard approximation is given as (Hirth and Lothe, 1982): $W_c\approx Db^2/2$.

The work A of the shear stress, spent to generation of the dislocation, is calculated in the standard way (Mura, 1968) as the work spent to movement of the dislocation from the crack tip to its final position (shown in Fig. 1). At the same time, in the case under our study, one should take into account the fact that the dislocation is generated through local shear events occurring in the GB. In doing so, we should take into consideration the additional term characterizing the resistance of the GB to plastic shear (local shear events) resulting in the formation of the dislocation. In a first approximation, we assume that the resistance of the GB to plastic shear is described as the friction force which acts on the moving dislocation and is equal by magnitude to $b\tau_0$, where τ_0 is the threshold shear stress for the intergrain sliding. According to this assumption,

plastic shear in the GB occurs, if the local shear stresses $\geqslant \tau_0$ at every point of the boundary. Then, the work A is represented in the following form:

$$A = b\int_0^r \sigma_{r\theta}^{K_I}(r_0,\theta)d\rho - b\tau_0 r_0, \qquad \sigma_{r\theta}^{K_I}(r,\theta) \geq \tau_0. \tag{7}$$

Here $\sigma_{r\theta}^{K_I}(r,\theta)$ is the stress tensor component (written in the polar coordinate system (r,θ) with the origin at the crack tip; see Fig. 1) created by the constant external one-axis tensile load in the vicinity of the crack tip and given by (Panasyuk, 1988)

$$\sigma_{r\theta}^{K_I}(r_k,\theta) = \frac{K_I^\sigma \sin\theta\cos(\theta/2)}{2\sqrt{2\pi r_k}}. \tag{8}$$

The inequality $\sigma_{r\theta}^{K_I}(r,\theta) \geqslant \tau_0$ gives the necessary condition for intergrain sliding in the plane making the angle θ with the coordinate axis Ox, in the interval $0 < r < r_0$. After substitution of formula (8) and (7) and subsequent integration, one finds:

$$A = br_0\left(\frac{K_I^\sigma \sin\theta\cos(\theta/2)}{\sqrt{2\pi r_0}} - \tau_0\right), \quad K_I^\sigma \geqslant \frac{\tau_0\sqrt{8\pi r_0}}{\sin\theta\cos(\theta/2)}. \tag{9}$$

Then, with formulas (6) and (9) as well as the expression for W_c, we obtain the following formula for the characteristic energy change ΔW:

$$\Delta W = \frac{Db^2}{2}\left(\ln\frac{r_0}{r_c} + 1\right) - br_0\left(\frac{K_I^\sigma \sin\theta\cos(\theta/2)}{\sqrt{2\pi r_0}} - \tau_0\right), \quad K_I^\sigma \geqslant \frac{\tau_0\sqrt{8\pi r_0}}{\sin\theta\cos(\theta/2)}. \tag{10}$$

From the condition $\partial(\Delta W)/\partial b = 0$ of the minimum of the energy change ΔW one finds the following expression for the dislocation Burgers vector magnitude b:

$$b = \frac{(1-\nu)\sqrt{2\pi r_0}(K_I^\sigma \sin\theta\cos(\theta/2) - \tau_0\sqrt{2\pi r_0})}{G[\ln(r_0/r_c)+1]}, \quad K_I^\sigma \geqslant \frac{\tau_0\sqrt{8\pi r_0}}{\sin\theta\cos(\theta/2)}. \tag{11}$$

With formulas (4) and (11), we express the intensity factors k_I^d and k_{II}^d of the dislocation-induced stresses through K_I^σ. After substitution of formulas (4) and (11) as well as the equation $K_I^\sigma = K_{IC}^*$ into formula (3), we obtain the following equation for the critical value of the stress intensity factor K_{IC}^*:

$$PK_{IC}^{*2} + QK_{IC}^* + R = 0, \tag{12}$$

where

$$P = 8(\ln(r_0/r_c)+1)^2 - \sin^2\theta\cos^2(\theta/2)[24\ln(r_0/r_c) + 3\cos 2\theta - 4\cos\theta + 17], \tag{13}$$

$$Q = 2\tau_0\sqrt{2\pi r_0}\sin\theta\cos^2(\theta/2)[12\ln(r_0/r_c) + 3\cos 2\theta - 4\cos\theta + 5], \tag{14}$$

$$R = 8\pi r_0\tau_0^2\cos^2(\theta/2)[5 - 3\cos\theta] - 64\pi D\gamma(\ln(r_0/r_c)+1)^2. \tag{15}$$

Analysis of Eq. (12) shows that the equation always has a positive solution given as:

$$K_{IC}^* = \frac{-Q + \sqrt{Q^2 - 4PR}}{2P}. \tag{16}$$

Let us calculate the effective fracture toughness K_{IC}^* in the exemplary cases of nanocrystalline metals Al and Ni as well as nanocrystalline ceramic 3C–SiC (the cubic phase of silicon carbide). In doing so, we will use the following values of the parameters G, ν and γ. For Ni, we put (Hirth and Lothe, 1982) $G = 73$ GPa, $\nu = 0.34$ and $\gamma = 1.725$ J/m^2. For Al, we set (Hirth and Lothe, 1982) $G = 27$ GPa, $\nu = 0.34$ and $\gamma = 1$ J/m^2. For 3C–SiC, we get: $G = 217$ GPa, $\nu = 0.23$ (Ding et al., 2004) and $\gamma = 1.5$ J/m^2 (Mehandru and Anderson, 1990). The dislocation core radius is taken as $r_c \approx 0.1$ nm for all the materials. This value is close to typical values of the Burgers vector magnitude of the dislocation, resulting from our calculations (see below).

With formulas (13)–(16), the effective fracture toughness K_{IC}^* depends on the threshold shear stress τ_0 for the intergrain sliding. For metals, the value of the stress τ_0 is commonly very low. For instance, in the case of Al, the stress τ_0 does not exceed 4 MPa (Du et al., 2008). In these circumstances, it is a good approximation to take $\tau_0 = 0$, for both Al and Ni. With formulas (13)–(16) in the case of $\tau_0 = 0$, one finds that the ratio $K_{IC}^*/K_{IC} = 2\sqrt{2/P}[\ln(r_0/r_c)+1]$ does not depend on the material parameters G, ν and γ. In other words, this ratio is in practice identical, for all materials (in particular, metals) characterized by low values of the threshold shear stress τ_0.

In the case of nanocrystalline ceramic 3C–SiC with amorphous GBs, we take $\tau_0 = \tau_a$, where τ_a is the flow stress for the amorphous SiC phase. In general, τ_a is highly sensitive to both temperature and strain rate. For very low temperatures (close to $T = 0$ K) and/or high strain rates, athermal plastic deformation occurs. Following experiments (Khakani et al., 1994), the microhardness H_V of amorphous SiC is around 30 GPa. This value of H_V, according to the standard relation $\tau_f \approx H_V/6$ between H_V and athermal flow stress τ_f (Veprek et al., 2003), corresponds to the athermal flow stress $\tau_a = 5$ GPa of amorphous SiC. The stress level significantly decreases with rising temperature and/or decreasing strain rate, in which case thermally-assisted

deformation occurs. In our following consideration concerning thermally-assisted deformation, for definiteness, we will take τ_a = 1 GPa.

The dependences of the ratio K^*_{IC}/K_{IC} on the angle θ and the distance r_0 between the dislocation and the crack tip are presented as a map in Fig. 2, for nanocrystalline Al or Ni (Fig. 2a) and 3C–SiC (Fig. 2b). The map in Fig. 2a corresponds not only to Al and Ni, but also to any other materials with low values of the threshold shear stress τ_0 characterizing intergrain sliding. From this figure it follows that the local fracture toughness K^*_{IC} reaches its maximum value when the boundary plane (and thereby the Burgers vector of the dislocation) makes the angle of around 70° with the direction of crack growth. This is related to the fact that the stress $\sigma_{r\theta}$ has its maximum when the plane makes the angle ≈70° with the direction of crack growth. From Fig. 2 it follows that the dislocation formation leads to increase of K^*_{IC} by ≈30%, when $r_0 \approx 1$ nm. This effect is significant, but the increase in K^*_{IC} rapidly falls with increasing r_0 in the case of nanocrystalline 3C–SiC. For nanocrystalline Al and Ni, the increase in K^*_{IC} gradually decreases with increasing r_0. In general, as it follows from Fig. 2, the dislocation formation effect on fracture toughness K^*_{IC} is stronger in metals, compared to 3C–SiC with amorphous GBs. This is because in the latter case the threshold shear stress τ_0 for intergrain sliding is rather large.

In order to characterize the fracture toughness, one can use stresses and crack length instead of stress intensity factors. The crack length l is in the following relationship with the stress intensity factor (see, e.g., Panasyuk, 1988): $K^\sigma_I = \sigma_0\sqrt{\pi l/2}$. The results of our previous calculations can be directly re-formulated in terms of stresses and crack length in the examined situation where the crack length l is large enough ($l \gg r_0$). To do so, we put l = 100 nm. For l = 100 nm, the critical stress σ_{c0} needed to cause the catastrophic crack growth in the dislocation-free case (the critical stress for brittle fracture) is given as: $\sigma_{c0} = \sqrt{8G\gamma/[(1-\nu)\pi l]}$. That is, σ_{c0}≈1 GPa for Al, ≈2.2 GPa for Ni, and ≈3.3 GPa for 3C–SiC. The dislocation formation (Fig. 1) leads to increase of the critical stress σ_c by 10–30% (Fig. 2). For instance, in the case of Al, for θ = 70°, we have: $\sigma_c \approx 1.30$ GPa at r_0 = 2 nm; $\sigma_c \approx 1.23$ GPa at r_0 = 5 nm; and $\sigma_c \approx 1.20$ GPa at r_0 = 10 nm. In the case of Ni, for θ = 70°, we obtain: $\sigma_c \approx 2.83$ GPa at r_0 = 2 nm; $\sigma_c \approx 2.69$ GPa at r_0 = 5 nm; and $\sigma_c \approx 2.62$ GPa at r_0 = 10 nm. In the case of 3C–SiC, for θ = 70°, we get: $\sigma_c \approx 4.1$ GPa at r_0 = 2 nm; $\sigma_c \approx 3.9$ GPa at r_0 = 5 nm; and $\sigma_c \approx 3.8$ GPa at r_0 = 10 nm.

To summarize, in the situation where intergrain sliding in a nanocrystalline specimen near a crack tip is not accommodated, it results in formation of a dislocation at a triple junction nearest to the crack tip. The triple junction dislocation creates a stress field that relieves, in part, the high local stress concentrated near the crack tip. It was found that the non-acommodated intergrain sliding increases fracture toughness K_{IC} by 10–30% in nanocrystalline Al, Ni and 3C–SiC.

4. Crack blunting due to accommodated intergrain sliding and its effect on fracture toughness of nanocrystalline materials at intermediate temperatures

Let us consider the situation where intergrain sliding near a crack tip is effectively accommodated through GB-diffusion-controlled processes, first of all, climb of GB dislocations. Commonly, this situation comes into play at intermediate homologous temperatures at which GB diffusion is intensive but grain growth (destroying the nanocrystalline structure) is suppressed. Intensive GB diffusion enhances climb of GB dislocations that effectively accommodates intergrain sliding, as it is schematically shown in Fig. 3. At the first stage of the accommodation, a triple junction dislocation (produced by intergrain sliding; Fig. 3b) climbs along a GB adjacent to the triple junction (Fig. 3c). Then, a new dislocation is formed due to intergrain sliding at the triple junction located near the crack tip, and, as a result, the crack tip blunts (Fig. 3d). The processes of GB dislocation climb and intergrain-sliding-produced formation of GB dislocations consequently occur resulting in dramatic blunting of the crack (Fig. 3c–f).

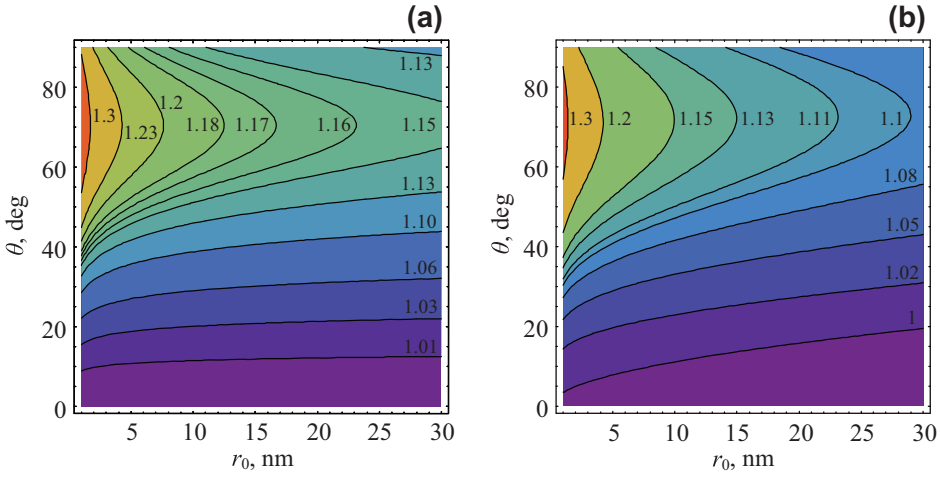

Fig. 2. Maps of the ratio K^*_{IC}/K_{IC} (as a function of the angle θ and distance r_0 between the crack tip and the dislocation) in the case of an edge dislocation located near a crack tip in (a) Al or Ni, and (b) SiC.

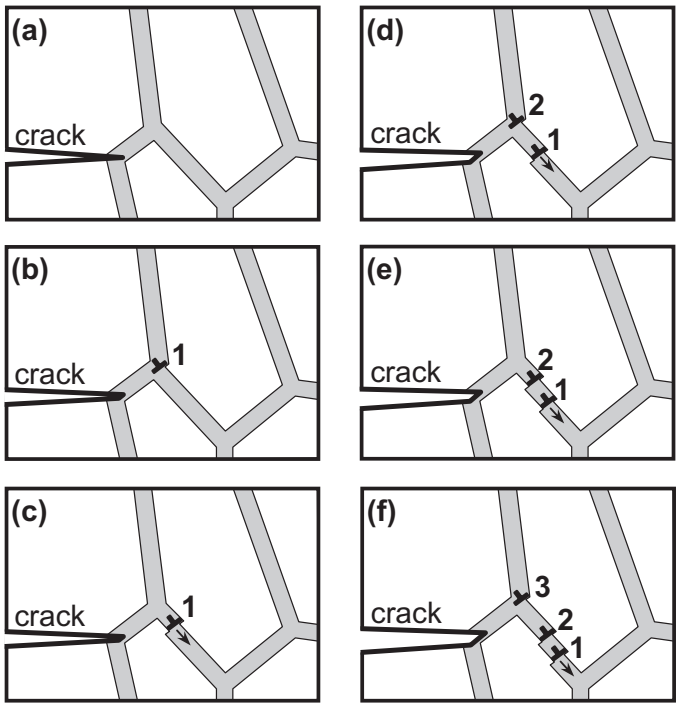

Fig. 3. Intergrain sliding is accommodated through climb of grain boundary dislocations. Intergrain sliding near a crack tip produces triple junction dislocations. These dislocations climb away, in which case intergrain sliding is enhanced and leads to the blunting of the crack.

Another scenario of GB-diffusion-controlled accommodation of intergrain sliding near a crack tip involves emission of lattice dislocations from triple junctions of GBs, as it is schematically shown in Fig. 4. In doing so, intergrain-sliding-produced dislocations at triple junctions of GBs transform into lattice dislocations that are emitted into grain interiors (Fig. 4).

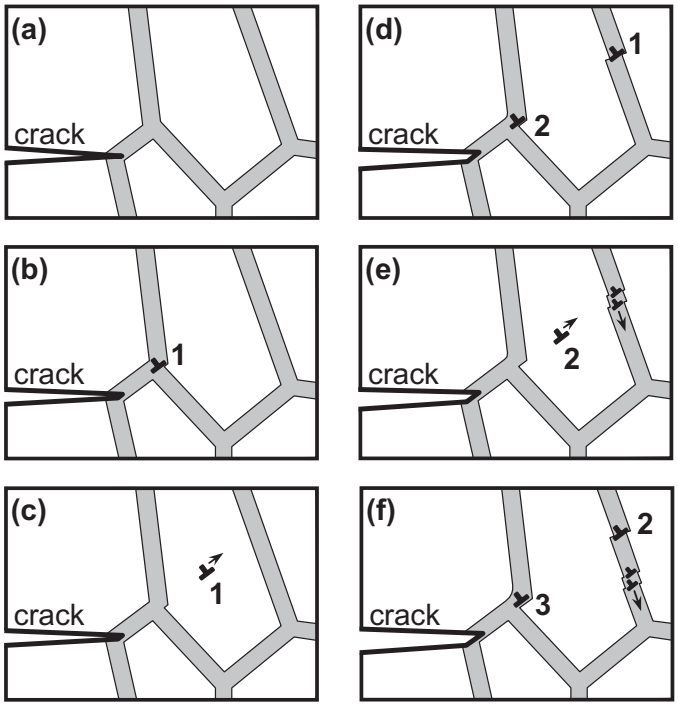

Fig. 4. Intergrain sliding is accommodated through both emission of lattice dislocation from triple junctions and following climb of grain boundary dislocations. Intergrain sliding near a crack tip produces triple junction dislocations that transform into moving lattice dislocations. The emission of these lattice dislocations from the triple junction leads to the blunting of the crack. The emitted lattice dislocations reach opposite grain boundary where these dislocations split into grain boundary dislocations that climb away.

The lattice dislocations reach a grain boundary (opposite to a triple junction emitting the dislocations) and transform into grain boundary dislocations (Fig. 4). Then the emitted dislocations create stress fields that suppress both further emission of lattice dislocations from the triple junction and thereby grain boundary sliding (Ruano et al., 2003; Langdon, 2006). However, when the GB dislocations climb far from the triple junction, the junction again becomes active as the lattice dislocation source. In these circumstances, intergrain sliding accommodated by lattice dislocation emission from triple junctions and further GB dislocation climb can result in dramatic blunting of the crack (Fig. 4).

The accommodation of intergrain sliding through emission of lattice dislocation from triple junctions (Fig. 4) can occur in nanocrystalline materials, if the Burgers vector magnitudes b of intergrain-sliding-produced dislocations is equal to or larger than the Burgers vector magnitude b_l for a perfect lattice dislocation. In this context, it is important to estimate typical values of b in nanocrystalline materials. Fig. 5 presents the dependences of the Burgers vector magnitude b on the angle θ and the distance r_0, for Al (Fig. 5a), Ni (Fig. 5b) and SiC (Fig. 5c). These dependences are shown as maps. The maps in Fig. 5 are calculated using formula (11) in the case of $K_I^{\sigma} = K_{IC}^{*}$. That is, these dependences show the critical magnitude b_c of the Burgers vector of the dislocation whose formation requires the external stress equal to the critical stress for growth of the crack having the dislocation in its vicinity. As a corollary, the dislocation Burgers vector magnitude b_c is the maximum magnitude at given values of r_0 and θ, because generation of the dislocation with the Burgers vector magnitude $b > b_c$ in the point (r_0, θ) requires the stress level exceeding the critical stress for crack growth. As it follows from Fig. 5, the typical values of the critical Burgers vector magnitude for SiC are of the order of 0.1 nm. For nanocrystalline Ni and Al, such values grow from around 0.2 nm to around 0.4 and 0.6 nm, respectively, when the distance r_0 (between the triple junction dislocation and the crack tip) increases from 1 to 30 nm. In particular, for $r_0 > 5$ nm, the critical Burgers vector magnitude b_c is larger than the Burgers vector magnitudes b_l for perfect lattice dislocations in Al (2.86 Å) and Ni (2.49 Å) (Fig. 5b). In these circumstances, intergrain sliding accommodated through the dislocation emission and associated GB dislocation (Fig. 4) can occur.

When the intergrain sliding (Fig. 4) comes into play, for $b_c \geqslant b_l$, there is a limit $b_{emission}$ of the Burgers vector magnitude of the Volterra dislocation produced by intergrain sliding. The limit $b_{emission}$ represents the minimum Burgers vector magnitude of the Volterra dislocation, at which the lattice dislocation emission into a grain interior (Fig. 4) occurs. In general, $b_{emission}$

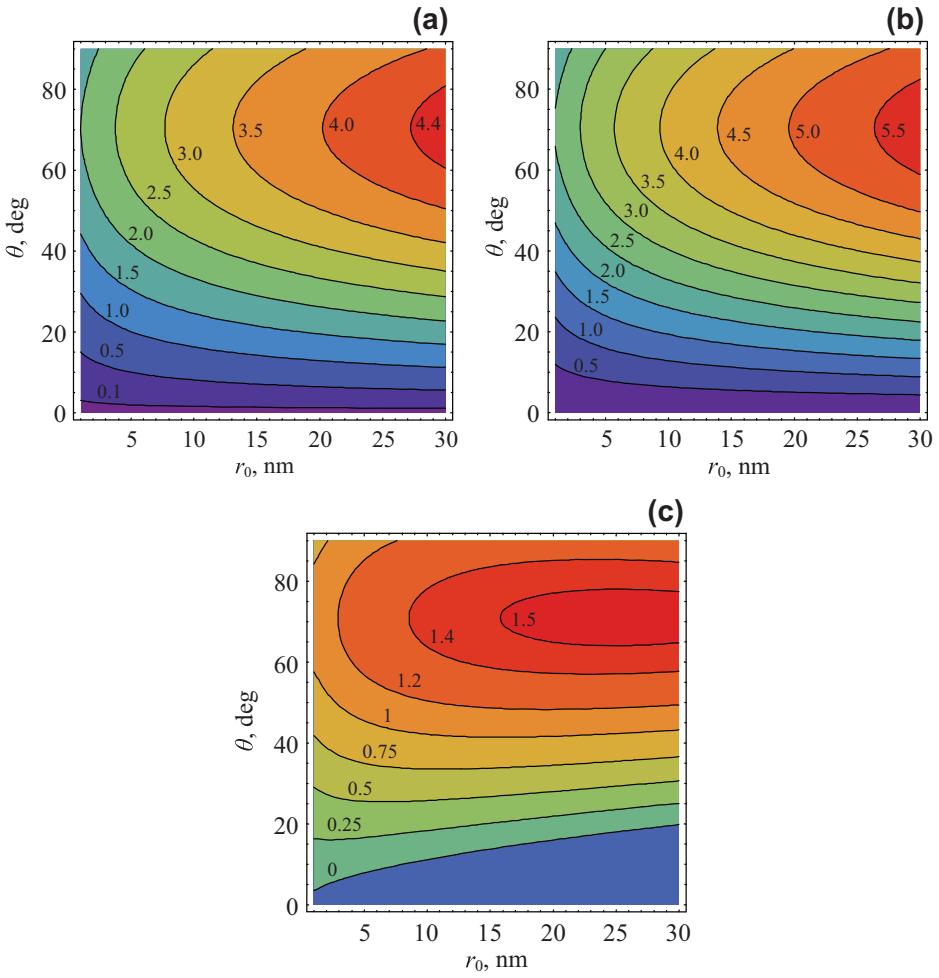

Fig. 5. Maps of the critical magnitude b_c of the dislocation Burgers vector (as a function of the angle θ and distance r_0 between the crack tip and the dislocation) located near a crack tip in (a) Al, (b) Ni and (c) SiC (for details, see text).The values of b_c are given in angstroms.

ranges rather widely, because the dislocation emission process strongly depends on several factors (first of all, crystallography of the adjacent grain and the applied stress). An exact calculation of $b_{emission}$ represents a separate problem which is beyond the scope of this paper. Instead, here we have used the lowest value of $b_{emission}$ ($b_{emission} = b_l$) as an input in calculations of the lowest bound for fracture toughness enhancement due to the Volterra dislocation generation. The results of the calculations are presented in Fig. 6, for nanocrystalline Al and Ni. As it follows from Figs. 2 and 6, the existence of the limit for the Burgers vector magnitude of the Volterra dislocation modifies the dependences of the ratio K^*_{IC}/K_{IC} on the angle θ and the distance r_0 between the crack tip and the dislocation. However, the effect in question is not dramatic.

At the same time, when intergrain sliding near a crack tip is effectively accommodated through climb of GB dislocations (without or with dislocation emission from triple junctions; see Figs. 3 and 4, respectively), essential crack blunting can occur, and its effects on crack growth can be significant. In the rest of this section, we consider the situation where crack blunting plays the dominant role in hampering crack growth and estimate the effect of crack blunting on the fracture toughness of nanocrystalline metals.

To do so, we will use the approach suggested by Beltz et al. (1999). Following Beltz et al. (1999) and Huang and Li (2004), we model the crack as an elongated ellipse with a curvature radius ρ at the crack tip, which is much smaller than the crack length (Fig. 7).

Following Beltz et al. (1999), we also assume that the growth of the blunt crack is possible if the tensile stress σ_{tip} at the crack tip, normal to the crack plane, reaches some critical value σ_p ($\sigma_{tip} = \sigma_p$). The stress σ_{tip} at the crack tip follows as (Creager and Paris, 1967):

$$\sigma_{tip} = \frac{2K_I^\sigma}{\sqrt{\pi\rho}}, \tag{17}$$

where K_I^σ is the generalized stress intensity factor (Huang and Li, 2004) assuming that the ellipse is replaced by a sharp crack with a translation of the crack tip at the curvature center.

Within the macroscopic description that does not consider in detail what happens at the crack tip, the crack grows if $K_I^\sigma = K^*_{IC}$. Combining this with the relation $\sigma_{tip} = \sigma_p$ and formula (17), we obtain:

$$K^*_{IC} = \frac{\sigma_p\sqrt{\pi\rho}}{2}. \tag{18}$$

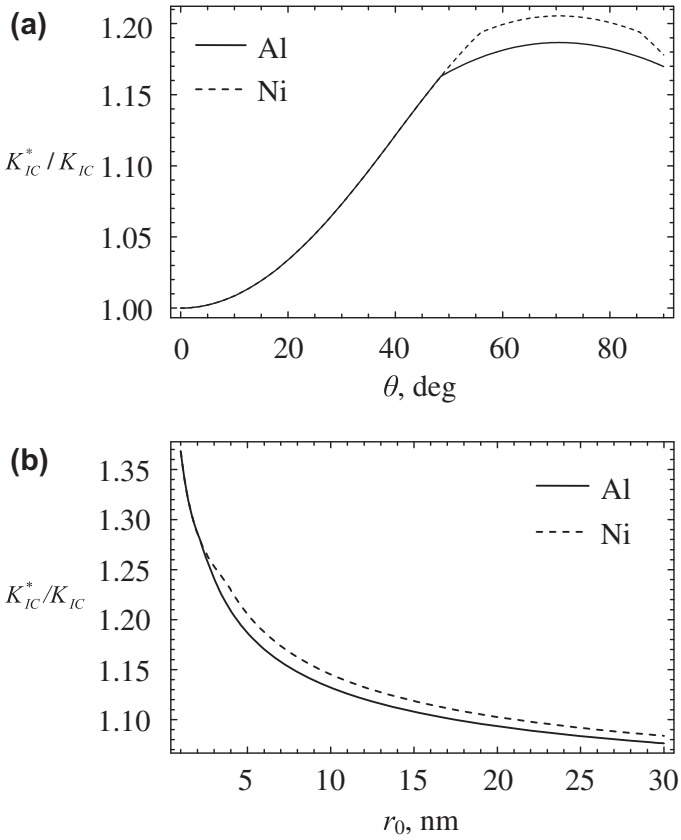

Fig. 6. Dependence of the ratio K^*_{IC}/K_{IC}, in the case of an edge Volterra dislocation whose Burgers vector has a limit $b_{emission} = b_l$ (for details, see text) in Al and Ni (solid and dashed curves, respectively), on (a) the angle θ made by the Burgers vector (or boundary plane) with the crack growth direction, for $r_0 = 5$ nm; and (b) on the distance r_0 between the crack tip and the dislocation, for $\theta = 70°$.

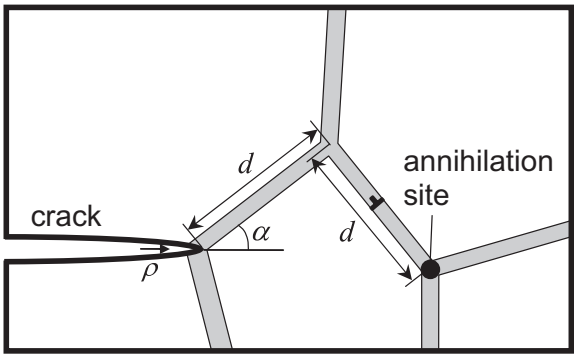

Fig. 7. Dislocation climb near the tip of a blunt crack.

Formula (18) is valid, when ρ is larger than some critical radius ρ_c at which the crack tip can be considered as curved. In the case of $\rho = 0$ (sharp crack), we will use the formula (see above) $K^*_{IC} = \sqrt{4G\gamma/(1-\nu)}$.

Following Beltz et al. (1999), we define ρ_c by the equality

$$\sqrt{4G\gamma/(1-\nu)} = \frac{\sigma_p\sqrt{\pi\rho_c}}{2}, \tag{19}$$

which gives: $\rho_c = 16G\gamma/[\pi(1-\nu)\sigma_p^2]$, and put

$$K^*_{IC} = \begin{cases} \sqrt{4G\gamma/(1-\nu)}, & \rho < \rho_c, \\ \frac{\sigma_p\sqrt{\pi\rho}}{2}, & \rho > \rho_c. \end{cases} \tag{20}$$

Now let us relate the value of K^*_{IC} with plastic deformation ε that occurs after the onset of intergrain sliding near the crack tip. We assume that the process of intergrain sliding is controlled by consequent climb of GB dislocations (Fig. 3) followed by their annihilation at an annihilation site. In this case, the crack tip curvature radius ρ can be estimated as: $\rho \approx (Nb_{GB}/2)\sin\alpha$, where $b_{GB} \approx 0,1$ nm is the Burgers vector of climbing GB dislocations and N is the number of GB dislocations that have climbed from the GB along which intergrain sliding occurs to an annihilation site.

In the case of a constant tensile stress σ normal to GB, the dislocation climb velocity v_c is given by (Friedel, 1964)

$$v_c = (D_{GB}/h)\{\exp[\sigma b^3_{GB}/(kT)] - 1\}, \tag{21}$$

where D_{GB} is the GB diffusion coefficient, h is the climbing distance to the annihilation site, T is the absolute temperature, and k is the Boltzmann constant.

Let us extend formula (21) for our case of varying σ. As a first approximation, for a rough estimate of the dependence $K^*_{IC}(\varepsilon)$, we calculate the average climb velocity through replacement of σ by $\bar\sigma$ in formula (21), where $\bar\sigma$ is the stress component, created by the applied load near the crack tip, normal to the examined GB (along which dislocation climb proceeds) and averaged over the dislocation climb way. Also, we focus on the situation where $\bar\sigma b^3_{GB}/(kT) < 1/2$, in which case $\exp[\bar\sigma b^3_{GB}/(kT)] - 1 \approx \bar\sigma b^3_{GB}/(kT)$.

For simplicity, hereafter we put $h = d \gg \rho$. That is, the GB annihilation site is located at a triple junction adjacent to the GB along which dislocation climb proceeds (Fig. 7). Then the average stress $\bar\sigma$ can be calculated using the expressions (e.g., Panasyuk, 1988) for the stress field created by an applied load near a mode I crack as: $\bar\sigma \approx (K^\sigma_I/\sqrt{2\pi d})f(\alpha)$, where

$$f(\alpha) = \int_0^1 (u^2+1)^{-1/4}\cos(\theta_0/2)[1 + \sin(\theta_0/2)\sin(2\alpha - 3\theta_0/2)]du, \tag{22}$$

and $\theta_0 = \alpha - \arctan u$.

The time necessary for a dislocation to climb the distance d towards the annihilation site is $t_a = d/v_c$. The number N of dislocations that climbed to the annihilation site during time t is $N = t/t_a$. In turn, the crack tip curvature radius after the climb of N dislocations can be estimated as: $\rho = (b_{GB}/2)N\sin\alpha$. Substitution of the expressions for N, t_a, v_c and $\bar\sigma$ into the latter relation for ρ yields:

$$\rho(t) = \frac{D_{GB}b^4 f(\alpha)\sin\alpha t}{2d^2\sqrt{2\pi d}kT}K^\sigma_I. \tag{23}$$

At $K^\sigma_I = K^*_{IC}$, ρ is related to K^*_{IC} by formula (24). Substituting the relation $K^\sigma_I = K^*_{IC}$ and formula (23) to formula (20) and taking into account that $t = \varepsilon/\dot\varepsilon$, one obtains:

$$K^*_{IC} = \max\left\{\frac{\pi\sigma_p^2 b^4 D_{GB} f(\alpha)\sin\alpha}{8d^2\sqrt{2\pi d}kT\dot\varepsilon}\varepsilon, \sqrt{4G\gamma/(1-\nu)}\right\}. \tag{24}$$

Let us estimate K^*_{IC} for Al. To do so, we will use the following parameter values: σ_p = 9.06 GPa, γ = 0.56 J/m^2 (Beltz et al. (1999) and references therein) and the values of G and ν specified above. We also put $\alpha = \pi/6$ and d = 15 nm. For the GB diffusion coefficient D_{GB} we employ the Arrhenius formula (e.g., Sutton and Balluffi, 1996) $D_{GB} = D_{b0}\exp[-Q_b/(RT)]$, where R is the universal gas constant, and set the following typical values of the GB diffusion activation energy Q_b and pre-factor D_{b0} (Kwieciski and Wyrzykowski, 1991): Q_b = 46.2 kJ/mol and $D_{b0} = 2.2 \cdot 10^{-9}$ m^2/s.

The dependences $K^*_{IC}(\varepsilon)$ for Al are shown in Fig. 8a, for various values of temperature T and strain rate $\dot{\varepsilon}$. As it follows from Fig. 8a, for relatively high temperatures and small strain rates (see curves 1, 2 and 3 in Fig. 8a), dislocation climb rapidly accommodates intergrain sliding. This results in significant crack blunting and, as a consequence, can lead to dramatic enhancement of fracture toughness. For example, at $\varepsilon = 0.03$, an increase in K^*_{IC} due to crack blunting is 155% and 26% for the cases shown in curves 1 and 2, respectively. These values of K^*_{IC} correspond to the crack tip radii ρ of 9.3 nm and 2.3 nm, respectively. (Also, in the exemplary case with $\varepsilon = 0.03$ and crack length l = 400 nm, the values of K^*_{IC} for the cases shown in curves 1, 2 and 3 correspond to the values of the critical load $\sigma_{0c} = K^*_{IC}/\sqrt{\pi l/2}$ equal to 977 GPa, 482 MPa and 381 MPa, respectively. Apparently, the value of σ_{0c} = 977 MPa is much higher than typical values of the flow stress of nanocrystalline Al.) At the same time, for small temperatures and/or high strain rates, dislocation climb is too slow to sufficiently accommodate intergrain sliding, and so the enhancement of fracture toughness due to crack blunting is not significant (see curve 4 in Fig. 8a).

For a specified crack length l, the stress intensity factor $K^\sigma_I = \sigma_0\sqrt{\pi l/2}$ scales with the applied stress σ_0 and increases with ε. Thus, catastrophic crack propagation can occur if at some ε, K^σ_I reaches its critical value K^*_{IC}. In order to illustrate it, consider the case of designated temperature T and strain rate $\dot{\varepsilon}$. For this case, we employ the following model stress-strain dependence: $\sigma_0(\varepsilon) = A(\varepsilon + \varepsilon_0)^n$, where ε_0 is the deformation corresponding to the onset of intergrain sliding and dislocation climb near the crack tip, and A and n are model parameters. Using this dependence, we obtain: $K^\sigma_I(\varepsilon) = A\sqrt{\pi l/2}(\varepsilon + \varepsilon_0)^n$.

The plots of the dependences $K^\sigma_I(\varepsilon)$ are shown in Fig. 8b for l=400 nm, $\varepsilon_0 = 0.02$, n = 0.4, and two different values of the parameter A (A = 1.3 GPa and A = 1.5 GPa; see the lower and upper solid lines, respectively). For comparison, the dependence $K^*_{IC}(\varepsilon)$ is also shown in this figure as a dashed line, for the case of nanocrystalline Al deformed at T = 353 K and $\dot{\varepsilon} = 8 \cdot 10^{-3}$ s^{-1}. (This dependence is identical to that shown in curve *2* in Fig. 8a.) As is seen in Fig. 8b, depending on the parameter values, two situations can take place. If the flow stress is large enough, the curve $K^\sigma_I(\varepsilon)$ intersects the curve $K^*_{IC}(\varepsilon)$ at some critical strain ε_c and critical stress σ_{0c}. At this critical strain and stress, the crack starts to propagate, which results in the fracture of the nanocrystalline solid. For the model case shown in Fig. 8b, the critical stress σ_{0c} is approximately equal to 380 MPa. In contrast, if the flow stress of the deformed solid is sufficiently small, the curve $K^\sigma_I(\varepsilon)$ always lies below

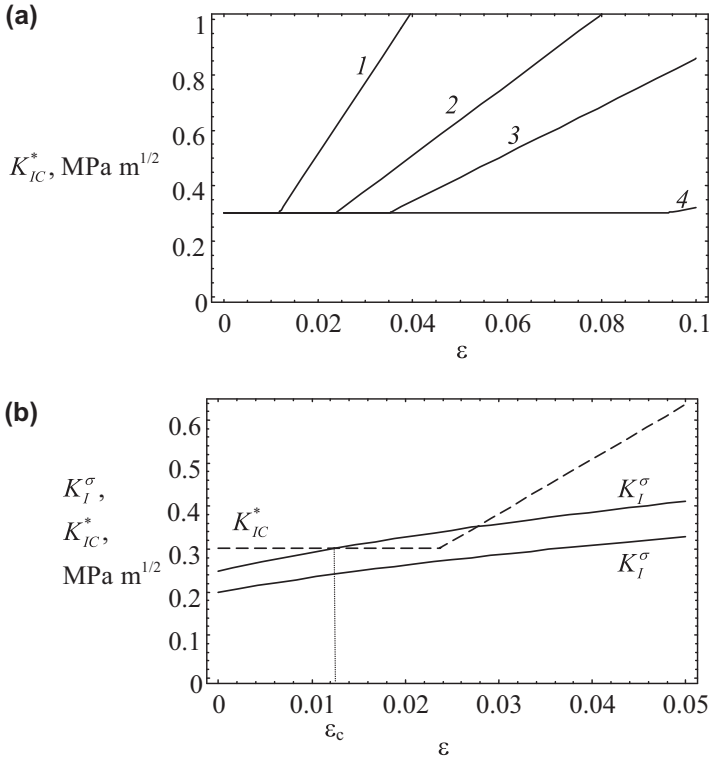

Fig. 8. Stress intensity factor K^σ_I and critical stress intensity factor K^*_{IC} for nanocrystalline Al as functions of plastic strain ε after the onset of intergrain sliding near the crack tip. (a) Dependences $K^*_{IC}(\varepsilon)$ for T = 323 K and $\dot{\varepsilon} = 10^{-3}$ s^{-1} (curve 1), T = 353 K and $\dot{\varepsilon} = 8 \cdot 10^{-3}$ s^{-1} (curve 2), T = 323 K and $\dot{\varepsilon} = 3 \cdot 10^{-3}$s^{-1} (curve 3), and T = 323 K and $\dot{\varepsilon} = 8 \cdot 10^{-3}$ s^{-1} (curve 4). (b) Dependences $K^\sigma_I(\varepsilon)$ (solid lines) and $K^*_{IC}(\varepsilon)$ (dashed line), for A=1.3 GPa and 1.5 GPa (lower and upper solid line, respectively), T = 353 K and $\dot{\varepsilon} = 8 \cdot 10^{-3}$ s^{-1}.

the curve $K^*_{IC}(\varepsilon)$. In this case, intergrain sliding accommodated by dislocation climb completely suppresses crack propagation at any strain ε.

As follows from formula (24), if $K^*_{IC} > K_{IC}$, the critical stress intensity factor K^*_{IC} rapidly falls with an increase in grain size d (K^*_{IC} scales with d as $K^*_{IC} \sim d^{-5/2}$). The dependences of K^*_{IC} on grain size d for nanocrystalline Al deformed at $\dot{\varepsilon} = 10^{-3}$ s^{-1} and various temperatures T are shown in Fig. 9, for $\varepsilon = 0.03$. Fig. 9 clearly demonstrates that the effect of crack blunting on fracture toughness K^*_{IC} is essential only in the range of small grain size (that is, if grain size d is smaller than some critical value d_c). At $d = d_c$, fracture toughness reaches its limiting value K_{IC}, corresponding to the case of brittle fracture, and does not change with a further increase in d. As temperature T increases, the critical grain size d_c also increases, and for a specified grain size d an increase in K^*_{IC} with a decrease in d becomes much more pronounced. As grain size d increases, GB dislocation climb becomes too slow to fully accommodate intergrain sliding and can no more promote fast crack blunting and associated increase in fracture toughness K^*_{IC}.

5. Discussion. Concluding remarks

Thus, though most nanocrystalline materials have low ductility and low fracture toughness (see, e.g., reviews Mukherjee, 2002; Kumar et al., 2003a; Kuntz et al., 2004; Ovid'ko, 2005, 2007; Wolf et al., 2005; Meyers et al., 2006; Dao et al., 2007; Koch, 2007), there are experimental data showing enhancement of fracture toughness of several nanocrystalline ceramics (Bhaduri and Bhaduri, 1997; Kuntz et al., 2004; Zhao et al., 2004; Kaminskii et al., 2005; Pei et al., 2005) and nanocrystalline Ni (Mirshams et al., 2001), compared to that of their microcrystalline counterparts. The fracture toughness enhancement can be attributed to specific toughening mechanisms that operate in these nanocrystalline materials (due to large amounts of GBs and the nanoscale effects) and effectively "replace" the conventional toughening through the lattice dislocation emission from crack tips. Here we suggested theoretical models describing one such specific toughening mechanism, namely toughening through non-accommodated and accommodated intergrain sliding processes in nanocrystalline materials at low and intermediate temperatures, respectively. Within the first model, the non-accommodated intergrain sliding in the vicinities of crack tips in nanocrystalline materials at comparatively low temperatures results in formation of immobile non-crystallographic Volterra dislocations at triple junctions of GBs (Fig. 1). For nanocrystalline Al, Ni and 3C–SiC, from the force criterion for crack growth, we revealed that the effective fracture toughness K^*_{IC} increases by ~30% due to the dislocation produced by the non-accommodated intergrain sliding at a triple junction of GBs, when the distance r_0 between the dislocation and the crack tip is around 1 nm. This effect is significant, but the increase in K^*_{IC} rapidly falls with increasing r_0 in SiC (Fig. 2b). For nanocrystalline Al and Ni, the increase in K^*_{IC} gradually decreases with increasing r_0 (Fig. 2a). The discussed sensitivity of fracture toughness to the distance r_0 (Fig. 2) correlates with the toughness sensitivity to the grain size d, because the likelihood to have a triple junction closely located to a crack tip is large when the grain size is very low. (More than that, the distance r_0 is very close to the grain size in nanocrystalline materials with finest grains, in which cracks tend to propagate along GBs (Fig. 10).) In these circumstances, the role of intergrain sliding as a specific toughening mechanism is expected to be well pronounced in nanocrystalline metals and ceramics with finest grains.

In the case of intermediate temperatures, the intergrain sliding is effectively accommodated by diffusion-controlled climb of grain boundary dislocations and dislocation emission to the grain interior (Figs. 3 and 4). The accommodated intergrain sliding is capable of causing significant blunting of cracks in nanocrystalline materials, which can significantly increase (by a factor ranging from 1.1 to around 3, depending on temperature) fracture toughness and thus hamper crack growth. This effect is well pronounced in nanocrystalline materials with finest grains and diminishes dramatically when grain size d increases (Fig. 9). That is, the considered effect of the accommodated intergrain sliding is inherent precisely to nanocrystalline materials and does not operate in coarse-grained polycrystals.

With the results of this paper, the experimentally detected difference in fracture behavior between tough and brittle nanocrystalline materials can be attributed to the respectively effective and ineffective replacement of the conventional toughening mechanism (through lattice dislocation emission from crack tips that dominates in conventional polycrystals)

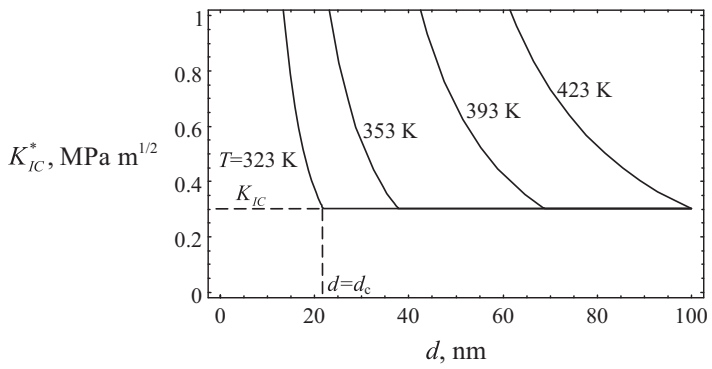

Fig. 9. Critical stress intensity factor K^*_{IC} for nanocrystalline Al as a function of grain size d.

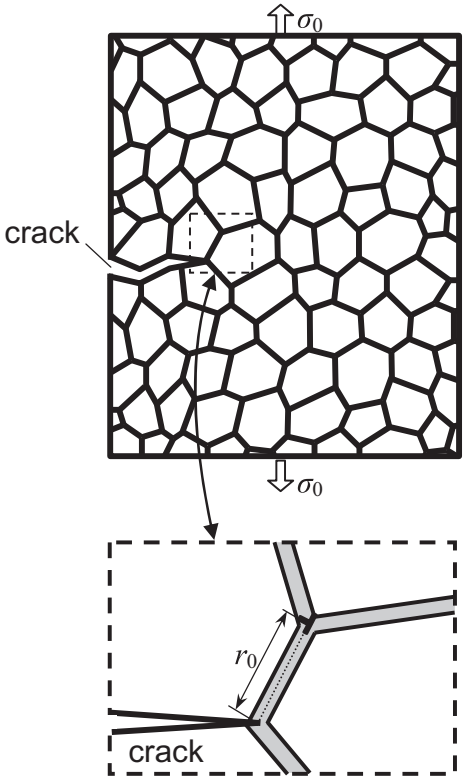

Fig. 10. Curved intergranular crack in a nanocrystalline solid with finest grains. The crack tip is located at a triple junction of grain boundaries. The stress concentration near the crack tip induces intergrain sliding that results in generation of a dislocation at another triple junction.

by alternative toughening mechanisms (in particular, intergrain sliding) in nanocrystalline materials. If alternative toughening mechanisms intensively operate in a nanocrystalline specimen, it shows enhanced toughness compared to that of its coarse-grained counterpart. In contrast, a nanocrystalline specimen has low fracture toughness, if alternative toughening mechanisms do not effective replace the conventional toughening mechanism.

The discussed difference in the fracture behavior of nanocrystalline materials is well illustrated by the experimental data (Mirshams et al., 2001) concerning crack growth in nanocrystalline Ni specimens (with grain size being around 20 nm) processed at different conditions. More precisely, Mirshams et al. (2001) reported that the crack growth resistivity of nanocrystalline nickel thin sheets at room temperature, in the cases of as-fabricated specimens and specimens after annealing at 373 K, exceeds the resistivity of coarse-grained polycrystalline nickel. In contrast, after annealing at 473 K, nanocrystalline Ni shows low crack growth resistivity, compared to that of coarse-grained Ni. These interesting experimental data are naturally explained in terms of sensitivity of intergrain sliding (and other alternative toughening mechanisms conducted by GBs) to the structure of GBs. Such boundaries in as-fabricated nanocrystalline metallic specimens are commonly non-equilibrium (Valiev and Alexandrov, 1999; Valiev et al., 2000; Huang et al., 2001; Valiev, 2004; Koch et al., 2007). They contain many excess GB dislocations, in which case intergrain sliding in as-fabricated nanocrystalline Ni specimens is enhanced. Annealing at comparatively low temperature, 373 K, does not dramatically change the non-equilibrium GB structures. Therefore, the non-accommodated intergrain sliding is still enhanced and effectively hampers crack growth in as-fabricated nanocrystalline Ni specimens and specimens after annealing at 373 K. In contrast, after annealing at 473 K, non-equilibrium GBs transform into equilibrium ones. This is because 473 K is close to characteristic temperature T_{GBD} at which intensive GB diffusion processes occur and cause extra GB dislocations to be annihilated. (For metals, T_{GBD} is around $0.3T_m$, where T_m is the melting temperature (Vladimirov, 1975). For Ni, $T_m = 1728$ K, and T_{GBD} is around 520 K.) In these circumstances, intergrain sliding and other alternative toughening mechanisms (conducted by GBs) are suppressed and hardly hamper crack growth in nanocrystalline Ni specimens after annealing at 473 K.

Acknowledgements

The work was supported, in part, by the National Science Foundation Grant CMMI #0700272, the Office of Naval Research (Grant N00014-1-07-0295), the Russian Foundation of Basic Research (Grant 08-01-00225-a), the Russian Academy of Sciences Program "Fundamental studies in nanotechnologies and nanomaterials", and the Federal Agency of Science and Innovations (Grants MK-1702.2008.1, MK-1702.2010.1).

References

Aifantis, E.C., 2009. Deformation and failure of bulk nanograined and UFG materials. Mater. Sci. Eng. A 503 (1), 190–201.
Argon, A.S., 1979. Plastic deformation in metallic glasses. Acta Metall. 27 (1), 47–58.
Ashby, M.F., Verall, R.A., 1973. Diffusion-accommodated flow and superplasticity. Acta Metall. 21 (2), 149–163.
Barai, P., Weng, G.J., 2009. Mechanics of very fine-grained nanocrystalline materials with contribution from grain interior, GB zone, and grain boundary sliding. Int. J. Plast. 25 (12), 2410–2434.
Beltz, G.E., Lipkin, D.M., Fischer, L.L., 1999. Role of crack blunting in ductile versus brittle response of crystalline materials. Phys. Rev. Lett. 82 (22), 4468–4471.
Bhaduri, S., Bhaduri, S.B., 1997. Enhanced low temperature toughness of Al_2O_3–ZrO_2 nano/nano composites. Nanostruct. Mater. 8 (6), 755–763.
Bobylev, S.V., Gutkin, M.Yu., Ovid'ko, I.A., 2006. Partial and split dislocation configurations in nanocrystalline metals. Phys. Rev. B 73 (6). Art. no. 064102.
Bobylev, S.V., Mukherjee, A.K., Ovid'ko, I.A., 2009. Emission of partial dislocations from amorphous intergranular boundaries in deformed nanocrystalline ceramics. Scr. Mater. 60 (1), 36–39.
Bobylev, S.V., Ovid'ko, I.A., 2009. Nanodisturbances in deformed nanowires. Phys. Rev. Lett. 103 (13) (Art. no. 135501).
Capolungo, L., Cherkaoui, M., Qu, J., 2007. On the elastic–viscoplastic behavior of nanocrystalline materials. Int. J. Plast. 23 (4), 561–591.
Chen, M., Ma, E., Hemker, K.J., Sheng, H., Wang, Y., Cheng, X., 2003. Deformation twinning in nanocrystalline aluminum. Science 300 (5623), 1275–1277.
Clarke, D.R., 1987. Grain boundaries in polycrystalline ceramics. Annu. Rev. Mater. Sci. 17, 57–74.
Conrad, H., Narayan, J., 2000. On the grain size softening in nanocrystalline materials. Scr. Mater. 42 (11), 1025–1030.
Creager, M., Paris, P.C., 1967. Elastic field equations for blunt cracks with reference to stress corrosion cracking. Int J. Fracture 3 (4), 247–252.
Cui, J.P., Hao, Y.L., Li, S.J., Sui, M.L., Li, D.X., Yang, R., 2009. Reversible movement of homogenously nucleated dislocations in β-titanium alloy. Phys. Rev. Lett. 102 (4). Art. no. 045503.
Dao, M., Lu, L., Asaro, R.J., De Hosson, J.T.M., Ma, E., 2007. Toward a quantitative understanding of mechanical behavior of nanocrystalline metals. Acta Mater. 55 (12), 4041–4065.
Demkowicz, M.J., Argon, A.S., Farkas, D., Frary, M., 2007. Simulation of plasticity in nanocrystalline silicon. Philos. Mag. 87 (28), 4253–4271.
Ding, Z., Zhou, S., Zhao, Y., 2004. Hardness and fracture toughness of brittle materials: a density functional theory study. Phys. Rev. B 70 (18). Art. no. 184117.
Dominguez-Rodriguez, A., Gomez-Garcia, D., Zapata-Solvez, E., Chen, J.Z., Chaim, R., 2007. Making ceramics ductile at low homologous temperatures. Scr. Mater. 56 (2), 89–91.
Du, N., Bower, A.F., Krajewski, P.E., Taleff, E.M., 2008. The influence of a threshold stress for grain boundary sliding on constitutive response of polycrystalline Al during high temperature deformation. Mater. Sci. Eng. A 494 (1-2), 86–91.
Ebrahimi, F., Liscano, A.J., Kong, D., Zhai, Q., Li, H., 2006. Fracture of bulk face centered cubic (FCC) metallic nanostructures. Rev. Adv. Mater. Sci. 13 (1), 33–40.
Farkas, D., Curtin, W.A., 2005. Plastic deformation mechanisms in nanocrystalline columnar grain structures. Mater. Sci. Eng. A 412 (1-2), 316–322.
Farkas, D., Van Petegem, S., Derlet, P.A., Van Swygenhoven, H., 2005. Dislocation activity and nano-void formation near crack tips in nanocrystalline Ni. Acta Mater. 53 (11), 3115–3123.
Farrok, B., Khan, A.S., 2009. Grain size, strain rate, and temperature dependence of flow stress in ultra-fine grained and nanocrystalline Cu and Al: synthesis, experiment, and constitutive modeling. Int. J. Plast. 25 (5), 715–732.
Fedorov, A.A., Gutkin, M.Yu., Ovid'ko, I.A., 2003. Transformations of grain boundary dislocation pile-ups in nano- and polycrystalline materials. Acta Mater. 51 (4), 887–898.
Figueiredo, R.B., Kawasaki, M., Langdon, T.C., 2009. The mechanical properties of ultrafine-grained metals at elevated temperatures. Rev. Adv. Mater. Sci. 19 (1/2), 1–12.
Friedel, J., 1964. Dislocations. Pergamon Press, Oxford.
Gutkin, M.Yu., Ovid'ko, I.A., 2004. Plastic deformation in nanocrystalline materials. Springer, Berlin.
Gutkin, M.Yu., Ovid'ko, I.A., 2006. Special mechanism for dislocation nucleation in nanomaterials. Appl. Phys. Lett. 88 (21). Art. no. 211901.
Gutkin, M.Yu., Ishizaki, T., Kuramoto, S., Ovid'ko, I.A., 2006. Nanodisturbances in deformed Gum Metal. Acta Mater. 54 (9), 2489–2499.
Gutkin, M.Yu., Ishizaki, T., Kuramoto, S., Ovid'ko, I.A., Skiba, N.V., 2008a. Giant faults in deformed Gum Metal. Int. J. Plast. 24 (8), 1333–1359.
Gutkin, M.Yu., Ovid'ko, I.A., 2008. Homogeneous nucleation of dislocation loops in nanocrystalline metals and ceramics. Acta Mater. 56 (7), 1642–1649.
Gutkin, M.Yu., Ovid'ko, I.A., Skiba, N.V., 2008b. Crack-stimulated generation of deformation twins in nanocrystalline metals and ceramics. Philos. Mag. 88 (8), 1137–1151.
Hirth, J.P., Lothe, J., 1982. Theory of Dislocations. Wiley, New York.
Huang, M., Li, Z., 2004. Dislocation emission criterion from a blunt crack tip. J. Mech. Phys. Solids 52 (9), 1991–2003.
Huang, J.Y., Zhu, Y.T., Jiang, H., Lowe, T.C., 2001. Microstructures and dislocation configurations in nanostructured Cu processed by repetitive corrugation and straightening. Acta Mater. 49 (9), 1497–1505.
Hulbert, D.M., Jiang, D., Kuntz, J.D., Kodera, Y., Mukherjee, A.K., 2007. A low-temperature high-strain-rate formable nanocrystalline superplastic ceramic. Scr. Mater. 56 (12), 1103–1106.
Irwin, R.G., 1957. Analysis of stresses and strains near the end of a crack traversing a plate. J. Appl. Mech. 24 (3), 361–364.
Kaminskii, A.A., Akchurin, M.Sh., Gainutdinov, R.V., Takaichi, K., Shirakava, A., Yagi, H., Yanagitani, T., Ueda, K., 2005. Microhardness and fracture toughness of Y2O3-and Y3Al5O12-based nanocrystalline laser ceramics. Crystallogr. Rep. 50 (5), 869–873.
Khakani, M.A.E., Chaker, M., Jean, A., Boily, S., Kieffer, J.C., O'Hern, M.E., Ravet, M.F., Rousseaux, F., 1994. Hardness and Young's modulus of amorphous a-SiC thin films determined by nanoindentation and bulge tests. J. Mater. Res. 9 (1), 96–103.
Khan, A.S., Zhang, H., 2000. Mechanically alloyed nanocrystalline iron and copper mixture: behavior and constitutive modeling over a wide range of strain rates. Int. J. Plast. 16 (12), 1477–1492.
Khan, A.S., Zhang, H., Takacs, L., 2000. Mechanical response and modeling of fully compacted nanocrystalline iron and copper. Int. J. Plast. 16 (12), 1459–1476.
Khan, A.S., Suh, Y.S., Chen, X., Takacs, L., Zhang, H., 2006. Nanocrystalline aluminum and iron: mechanical behavior at quasi-static and high strain rates, and constitutive modeling. Int. J. Plast. 22 (2), 195–209.
Khan, A.S., Farrok, B., Takacs, L., 2008a. Compressive properties of Cu with different grain sizes: sub-micron to nanometer realm. J. Mater. Sci. 43 (9), 3305–3313.
Khan, A.S., Farrok, B., Takacs, L., 2008b. Effect of grain refinement on mechanical properties of ball-milled bulk aluminum. Mater. Sci. Eng. A 489 (1–2), 77–84.
Koch, C.C., 2007. Structural nanocrystalline materials: an overview. J. Mater. Sci. 42 (5), 1403–1414.
Koch, C.C., Ovid'ko, I.A., Seal, S., Veprek, S., 2007. Structural Nanocrystalline Materials: Fundamentals and Applications. Cambridge University Press, Cambridge.
Kumar, K.S., Suresh, S., Van Swygenhoven, H., 2003a. Mechanical behavior of nanocrystalline metals and alloys. Acta Mater. 51 (19), 5743–5774.
Kumar, K.S., Suresh, S., Chisholm, M.F., Norton, J.A., Wang, P., 2003b. Deformation of electrodeposited nanocrystalline nickel. Acta Mater. 51 (2), 387–405.
Kuntz, J.D., Zhan, G.-D., Mukherjee, A.K., 2004. Nanocrystalline-matrix ceramic composite for improved fracture toughness. MRS Bullet. 29 (1), 22–27.
Kwieciski, J., Wyrzykowski, J.W., 1991. Investigation of grain boundary self-diffusion at low temperatures in polycrystalline aluminium by means of the dislocation spreading method. Acta Metall. Mater. 39 (8), 1953–1958.
Langdon, T.G., 2006. Grain boundary sliding revisited: developments in sliding over four decades. J. Mater. Sci. 41 (3), 597–609.
Li, H., Ebrahimi, F., 2004. Transition of deformation and fracture behaviors in nanostructured face-centered-cubic metals. Appl. Phys. Lett. 84 (21), 4307–4309.
Li, H., Ebrahimi, F., 2005. Ductile-to-brittle transition in nanocrystalline metals. Adv. Mater. 17 (16), 1969–1972.

Liao, X.Z., Zhou, F., Lavernia, E.J., Srinivasan, S.G., Baskes, M.I., He, D.W., Zhu, Y.T., 2003. Deformation mechanism in nanocrystalline Al: partial dislocation slip. Appl. Phys. Lett. 83 (4), 632–634.
Lin, I.-H., Thomson, R., 1986. Cleavage, dislocation emission, and shielding for cracks under general loading. Acta Metall. 34 (2), 187–206.
Mehandru, S.P., Anderson, A.B., 1990. Structures and energetics for polar and nonpolar SiC surface relaxations. Phys. Rev. B 42 (14), 9040–9049.
Meyers, M.A., Mishra, A., Benson, D.J., 2006. Mechanical properties of nanostructured materials. Progr. Mater. Sci. 51 (4), 427–556.
Mirshams, R., Whang, S.H., Xiao, C.H., Yin, W.M., 2001. R-Curve characterization of the fracture toughness of nanocrystalline nickel thin sheets. Mater. Sci. Eng. A 315 (1), 21–27.
Mo, Y., Szlufarska, I., 2007. Simultaneous enhancement of toughness, ductility, and strength of nanocrystalline ceramics at high strain-rates. Appl. Phys. Lett. 90 (18). Art. no. 181926.
Mohamed, F.A., 2007. Interpretation of nanoscale softening in terms of dislocation accommodated boundary sliding. Metall. Mater. Trans. A 38 (2), 340–347.
Mohamed, F.A., Chauhan, M., 2006. Interpretation of the creep behavior of nanocrystalline Ni in terms of dislocation accommodated boundary sliding. Metall. Mater. Trans. A 37 (12), 3555–3567.
Monk, J., Hyde, B., Farkas, D., 2006. The role of partial grain boundary dislocations in grain boundary sliding and coupled grain boundary motion. J. Mater. Sci. 41 (23), 7741–7746.
Mukherjee, A.K., 2002. An examination of the constitutive equation for elevated temperature plasticity. Mater. Sci. Eng. A 322 (1–2), 1–22.
Mura, T., 1968. The continuum theory of dislocations. In: Herman, H. (Ed.), Advances in Materials Research, vol. III. Interscience, New York, pp. 1–108.
Ovid'ko, I.A., 2005. Deformation and diffusion modes in nanocrystalline materials. Int. Mater. Rev. 50 (2), 65–82.
Ovid'ko, I.A., 2007. Review on fracture processes in nanocrystalline materials. J. Mater. Sci. 42 (5), 1694–1708.
Ovid'ko, I.A., Sheinerman, A.G., Aifantis, E.C., 2008. Stress-driven migration of grain boundaries and fracture processes in nanocrystalline ceramics and metals. Acta Mater. 56 (12), 2718–2727.
Padmanabhan, K.A., Gleiter, H., 2004. Optimal structural superplasticity in metals and ceramics of microcrystalline- and nanocrystalline-grain sizes. Mater. Sci. Eng. A 381 (1-2), 28–38.
Panasyuk, V.V., 1988. In: Panasyuk, V.V. (Ed.), Fracture Mechanics and Strength of Materials, vol. 2. Naukova Dumka, Kiev. in Russian.
Pei, Y.T., Galvan, D., De Hosson, J.T.M., 2005. Nanostructure and properties of TiC/a-C:H composite coatings. Acta Mater. 53 (17), 4505–4521.
Ruano, O.A., Wadsworth, J., Sherby, O.D., 2003. Deformation of fine-grained alumina by grain boundary sliding accommodated by slip. Acta Mater. 51 (12), 3617–3634.
Sutton, A.P., Balluffi, R.W., 1996. Interfaces in Crystalline Materials. Oxford Science Publications, Oxford.
Szlufarska, I., Nakano, A., Vashista, P., 2005. A crossover in the mechanical response of nanocrystalline ceramics. Science 309 (5736), 911–914.
Valiev, R.Z., 2004. Nanostructuring of metals by severe plastic deformation for advanced properties. Nature Mater. 3 (8), 511–516.
Valiev, R.Z., Alexandrov, I.V., 1999. Nanostructured materials from severe plastic deformation. Nanostruct. Mater. 12 (1-4), 35–40.
Valiev, R.Z., Islamgaliev, R.K., Alexandrov, I.V., 2000. Bulk nanostructured materials from severe plastic deformation. Progr. Mater. Sci. 45 (2), 103–189.
Van Swygenhoven, H., Spaczer, M., Caro, A., 1999. Microscopic description of plasticity in computer generated metallic nanophase samples: a comparison between Cu and Ni. Acta Mater. 47 (10), 3117–3126.
Van Swygenhoven, H., Derlet, P.A., 2001. Grain-boundary sliding in nanocrystalline fcc metals. Phys. Rev. B 64 (22). Art. no. 224105.
Van Swygenhoven, H., Derlet, P.A., Hasnaoui, A., 2002. Atomic mechanism for dislocation emission from nanosized grain boundaries. Phys. Rev. B 66 (2). Art. no. 024101.
Veprek, S., Mukherjee, S., Karvankova, P., Mannling, H.-D., He, J.L., Moto, K., Prochazka, J., Argon, A.S., 2003. Limits to the strength of super- and ultrahard nanocomposite coatings. J. Vac. Sci. Technol. A 21 (3), 532–544.
Vladimirov, V.I., 1975. Einfuhrung in die Physikalishe Theorie der Plastizitat und Festigkeit. VEB Deutscher Verlag fur Grundstoffindustrie, Leipzig.
Volterra, V., 1907. Sur l'équilibre des corps élastiques multiplement connexes. Ann. Sci. Ecole Norm. Sup. 24, 401–517.
Wang, Y.M., Hodge, A.M., Biener, J., Hamza, A.V., Barnes, D.E., Liu, K., Nieh, T.G., 2005. Deformation twinning during nanoindentation of nanocrystalline Ta. Appl. Phys. Lett. 86 (10). Art. no.101915.
Warner, D.H., Sansoz, F., Molinari, J.F., 2006. Atomistic based continuum investigation of plastic deformation in nanocrystalline copper. Int. J. Plast. 22 (4), 754–774.
Weissmüller, J., Markmann, J., 2005. Deforming nanocrystalline metals: new insights, new puzzles. Adv. Eng. Mater. 7 (4), 202–207.
Wolf, D., Yamakov, V., Phillpot, S.R., Mukherjee, A.K., Gleiter, H., 2005. Deformation of nanocrystalline materials by molecular-dynamics simulation: relationship to experiments? Acta Mater. 53 (1), 1–40.
Wu, X.L., Zhu, Y.T., 2008. Inverse grain-size effect on twinning in nanocrystalline Ni. Phys. Rev. Lett. 101 (2). Art. no. 025503.
Xia, Z., Riester, L., Curtin, W.A., Li, H., Sheldon, B.W., Liang, J., Chang, B., Xu, J.M., 2004. Direct observation of toughening mechanisms in carbon nanotube ceramic matrix composites. Acta Mater. 52 (4), 931–944.
Xu, X., Nishimura, T., Hirosaki, N., Xie, R.-J., Yamamoto, Y., Tanaka, H., 2006. Superplastic deformation of nano-sized silicon nitride ceramics. Acta Mater. 54 (1), 255–262.
Yang, W., Wang, H.T., 2004. Mechanics modeling for deformation of nano-grained metals. J. Mech. Phys. Solids 54 (4), 875–889.
Yang, W., Wang, H.T., 2008. Brittle versus ductile transition of nanocrystalline metals, Int. J. Sol. Struct. 45 (13), 3897–3907.
Yang, F., Yang, W., 2009. Crack growth versus blunting in nanocrystalline metals with extremely small grain size. J. Mech. Phys. Solids 57 (2), 305–324.
Zhang, T.-Y., Li, J.C.M., 1991. Image forces and shielding effects of an edge dislocation near a finite length crack. Acta Metall. Mater. 39 (11), 2739–2744.
Zhao, Y., Qian, J., Daemen, L.L., Pantea, C., Zhang, J., Voronin, G.A., Zerda, T.W., 2004. Enhancement of fracture toughness in nanostructured diamond – SiC composites. Appl. Phys. Lett. 84 (8), 1356–1358.
Zhu, Y.T., Liao, X.Z., Valiev, R.Z., 2005. Formation mechanism of fivefold deformation twins in nanocrystalline face-centered-cubic metals. Appl. Phys. Lett. 86 (10). Art. no. 103112.
Zhu, Y.T., Wu, X.L., Liao, X.Z., Narayan, J., Mathaudhu, S.N., Kecskes, L.J., 2009. Twinning partial multiplication at grain boundary in nanocrystalline fcc metals. Appl. Phys. Lett. 95 (3). Art. no. 031909.